

## Accepted Manuscript

Title: Pharmacokinetic profile of PBRM in rodents, a first selective covalent inhibitor of 17 $\beta$ -HSD1 for breast cancer and endometriosis treatments

Authors: René Maltais, Alexandre Trottier, Jenny Roy, Diana Ayan, Nicolas Bertrand, Donald Poirier



PII: S0960-0760(17)30371-0  
DOI: <https://doi.org/10.1016/j.jsbmb.2017.12.007>  
Reference: SBMB 5084

To appear in: *Journal of Steroid Biochemistry & Molecular Biology*

Received date: 16-10-2017  
Revised date: 30-11-2017  
Accepted date: 13-12-2017

Please cite this article as: René Maltais, Alexandre Trottier, Jenny Roy, Diana Ayan, Nicolas Bertrand, Donald Poirier, Pharmacokinetic profile of PBRM in rodents, a first selective covalent inhibitor of 17 $\beta$ -HSD1 for breast cancer and endometriosis treatments, *Journal of Steroid Biochemistry and Molecular Biology* <https://doi.org/10.1016/j.jsbmb.2017.12.007>

This is a PDF file of an unedited manuscript that has been accepted for publication. As a service to our customers we are providing this early version of the manuscript. The manuscript will undergo copyediting, typesetting, and review of the resulting proof before it is published in its final form. Please note that during the production process errors may be discovered which could affect the content, and all legal disclaimers that apply to the journal pertain.

*Journal of Steroid Biochemistry and Molecular Biology (Revised)*

**Pharmacokinetic profile of PBRM in rodents, a first selective covalent inhibitor of 17 $\beta$ -HSD1 for breast cancer and endometriosis treatments**

René Maltais,<sup>1,§</sup> Alexandre Trottier,<sup>1,§</sup> Jenny Roy,<sup>1</sup> Diana Ayan,<sup>1</sup> Nicolas Bertrand<sup>2</sup> and Donald Poirier<sup>1,3,\*</sup>

<sup>1</sup> *Laboratory of Medicinal Chemistry, Endocrinology and Nephrology Unit, CHU de Québec - Research Center (CHUL, T4-42), Québec, QC, Canada*

<sup>2</sup> *Faculty of Pharmacy, Endocrinology and Nephrology Unit, CHU de Québec - Research Center (CHUL, T4-42), Québec, QC, Canada*

<sup>3</sup> *Department of Molecular Medicine, Faculty of Medicine, Université Laval, Québec, QC, Canada*

*§ These authors contributed equally to this work.*

Corresponding author:

Dr. Donald Poirier

Laboratory of Medicinal Chemistry

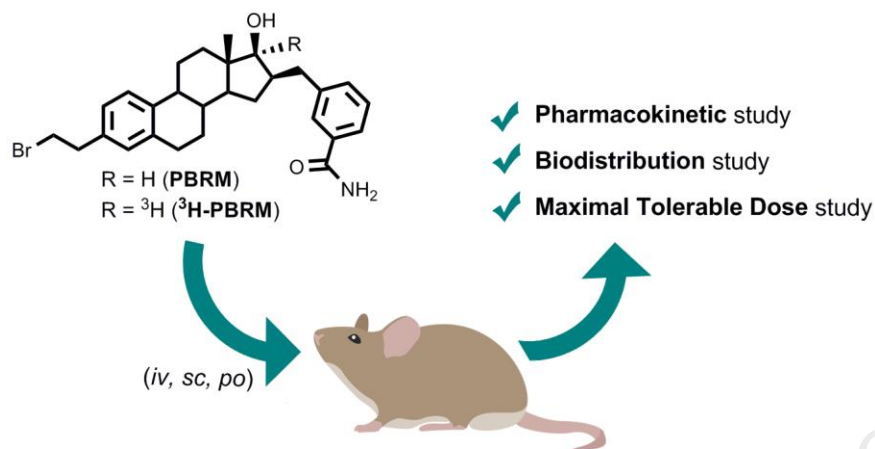
CHU de Québec - Research Center (CHUL, T4-42)

2705 Laurier Boulevard, Québec, QC, G1V 4G2, Canada

Phone: +1 418 654 2296; Fax: +1 418 654 2298

E-mail: [donald.poirier@crchul.ulaval.ca](mailto:donald.poirier@crchul.ulaval.ca)

## Graphical abstract



## Highlights

- Pharmacokinetics of PBRM, a potent 17 $\beta$ -HSD1 inhibitor, have been addressed in rodents
- High doses of PBRM are very well tolerated by mice for a period of several weeks
- Distribution of <sup>3</sup>H-PBRM shows a wide distribution among different mouse organs
- Metabolism studies of PBRM have identified PBRM-O as the sole metabolite
- The steroid derivative PBRM shows a good excretion profile and bioavailability

## Abstract

The development of a covalent inhibitor of 17 $\beta$ -hydroxysteroid dehydrogenase type 1 (17 $\beta$ -HSD1) is a promising approach for the treatment of hormone-dependent breast cancer and endometriosis. After reporting the steroid derivative PBRM as a first potent covalent inhibitor of 17 $\beta$ -HSD1 without estrogenic activity, we are now interested in studying its pharmaceutical behavior. The metabolism study in a human liver microsomal preparation showed a gradual transformation of PBRM into PBRM-O, an oxidized ketonic form of PBRM at position C17. Interestingly, PBRM-O also inhibits 17 $\beta$ -HSD1 and is not estrogenic in estrogen-sensitive T-47D cells. However, when PBRM was injected subcutaneously (*sc*) in mice, a very small proportion of PBRM-O was measured in a 24 h-time course experiment. A pharmacokinetic

study in mice revealed suitable values for half-life ( $T_{1/2} = 3.4$  h), clearance ( $CL = 2088$  mL/h.kg), distribution volume ( $V_z = 10.3$  L/kg) and absolute bioavailability ( $F = 65\%$ ) when PBRM was injected *sc* at 14.7 mg/kg. A good  $F$  value of 33% was also obtained when PBRM was given orally. A tritiated version of PBRM,  $^3\text{H}$ -PBRM, was synthesized and used for an *in vivo* biodistribution study that showed its gradual accumulation in various mouse tissues (peak at 6 h) followed by elimination until complete disappearance after 72 h. Elimination was found to occur in feces (93%) and urine (7%) as revealed by a mass balance experiment. PBRM was also evaluated for its toxicity in mice and it was found to be very well tolerated after weekly *sc* administration (30-405 mg/kg for 8 weeks) or by *po* administration (300-900 mg/kg for 4 weeks). Overall, these experiments represent important steps in the preclinical characterization of the pharmaceutical behavior of PBRM, as well as for its translation to clinical trials.

**Keywords:**  $17\beta$ -hydroxysteroid dehydrogenase type 1; steroid; irreversible inhibitor; pharmacokinetic; biodistribution; breast cancer; endometriosis.

## 1. Introduction

The development of covalent inhibitors as drugs for the treatment of cancer or endometriosis is a challenging task, particularly regarding selectivity over off-targets, and potential associated toxicity issues [1, 2]. However, at the same time, this class of compounds offers interesting potential benefits for new treatments such as a greater efficiency, lower frequency of administration, and a decreased risk of drug resistance [3]. These advantages have caused a resurgence of interest in the pharmaceutical industry over the last years, particularly for covalent drug candidates, bearing a low reactive chemical group that leads to higher specificity and a decreased risk of toxicity [4]. With that mindset, the characterization of a covalent inhibitor

regarding its pharmaceutical behavior is a crucial step to translating an interesting hit compound, with a promising *in vitro* profile, to a safe drug candidate for the initiation of clinical studies [5].

We have recently reported the development of the steroid derivative PBRM (Fig. 1), a selective covalent inhibitor of 17 $\beta$ -hydroxysteroid dehydrogenase type 1 (17 $\beta$ -HSD1) [6-8]. This enzyme is overexpressed in breast cancer and is responsible for the formation of estradiol (E2), the most potent estrogen in women, from the steroid precursor estrone (E1). In fact, this key steroidogenic enzyme represents a promising target to treat breast cancer, as well as other estrogen-dependent diseases, such as endometriosis and endometrial cancer [9-15]. At a molecular level, the 17 $\beta$ -HSD1 inhibitor PBRM possesses a 2-bromoethyl side chain at position C3 of an estratriene core, which represents a soft electrophilic reacting group. In fact, this halogenoalkyl group was very weakly reactive toward the nucleophilic residue of amino acids (AA) in a solution-phase laboratory experiment [16]. However, PBRM can be much more prone to react in a close confined proximity with a key nucleophilic AA residue [17], much like the imidazolyl group of His-221, which is found in the catalytic site of 17 $\beta$ -HSD1 [18].

The competitive irreversible inhibition by PBRM was shown to be very sensitive to the presence of His-221, but also to the nature of other proximal AA, thus supporting its selectivity of action [8, 16]. Therefore, this covalent inhibitor was found to be selective over a large variety of off-target key enzymes and receptors. It also showed an extended inactivation of 17 $\beta$ -HSD1 in two estrogen-sensitive cell lines (T-47D and JEG-3 cells) [16]. Furthermore, in an *in vivo* context, PBRM completely blocked the estrogen-dependent breast cancer tumor progression stimulated by E1 in a T-47D xenograft mouse cancer model [7]. Thus, this 17 $\beta$ -HSD1 inhibitor demonstrated a great *in vitro* profile as a covalent drug, as well as promising preliminary *in vivo* results for breast cancer treatment.

Herein, we report the results of investigation studies focusing on the metabolic profile and the pharmacokinetics of this candidate drug (PBRM), as well as its maximum tolerated dose. These data generated *in vitro* and in rodents are crucial to demonstrating the potential of this novel 17 $\beta$ -HSD1 inhibitor as a safe and valuable drug candidate to move on to the next step toward clinical trials [19].

## 2. Material and Methods

## 2.1. Chemical synthesis of PBRM, PBRM-O and <sup>3</sup>H-PBRM

### 2.1.1. Reagents, solvents, and apparatus

Reagents were purchased from Sigma-Aldrich (Oakville, ON, Canada) except for NaBT<sub>4</sub> (100 mCi in 2.5 mL of methanol (MeOH), 10.9 Ci/mmol) which was purchased from Perkin Elmer (Boston, MA, USA). Anhydrous dichloromethane (DCM) was obtained from Sigma-Aldrich, while ethyl acetate (EtOAc), hexanes, ethanol (EtOH) and MeOH were purchased from Fisher Scientific (Montréal, QC, Canada). Thin-layer chromatography (TLC) and flash-column chromatography were performed on 0.20-mm silica gel 60 F254 plates (E. Merck; Darmstadt, Germany) and with 230-400 mesh ASTM silica gel 60 (SiliCycle, Québec, QC, Canada), respectively. Nuclear magnetic resonance (NMR) spectra were recorded at 400 MHz for <sup>1</sup>H and 100.6 MHz for <sup>13</sup>C on a Bruker Avance 400 digital spectrometer (Billerica, MA, USA). The chemical shifts ( $\delta$ ) and coupling constants (J) were expressed in ppm and Hz, respectively. NMR data were referenced to acetone (2.06 ppm for <sup>1</sup>H NMR and 29.2 ppm for <sup>13</sup>C NMR). Low resolution-mass spectra (LR-MS) were recorded on a Shimadzu apparatus (Kyoto, Japan) equipped with an atmospheric pressure chemical ionization (APCI) source and data expressed in m/z. The HPLC purity was determined with a Shimadzu apparatus using a SPD-M20 photodiode array detector, an Alltima HP C18 column (250 mm x 4.6 mm, 5  $\mu$ m) and a gradient of solvents, from MeOH/water (70:30) to 100% MeOH over 30 min at a flow rate of 1 mL/min. The wavelength of the UV detector was selected at 190 nm.

### 2.1.2. PBRM

17 $\beta$ -HSD1 inhibitor PBRM, formally 3- $\{[(16\beta,17\beta)$ -3-(2-bromoethyl)-17-hydroxyestra-1,3,5(10)-trien-16-yl]methyl}benzamide, was synthesized as previously published [8].

### 2.1.3. PBRM-O

To a solution of PBRM (70 mg, 0.14 mmol) in DCM (3 mL) was added *N*-methylmorpholine-*N*-oxide (25 mg, 0.21 mmol), molecular sieves (70 mg) and tetrapropylammonium-perruthenate (7 mg, 0.02 mmol). The solution was stirred for 1 h at 0 °C and then for 3 h at room temperature. The resulting solution was directly purified by flash chromatography using DCM/MeOH (95:5) as eluent to give 36 mg (51%) of PBRM-O (3-

{[(16 $\beta$ )-3-(2-bromoethyl)-17-oxoestra-1,3,5(10)-trien-16-yl]methyl}benzamide).  $^1\text{H}$  NMR  $\delta_{\text{H}}$  (acetone- $d_6$ ): 0.77 (3 H, s), 1.26 – 1.61 (6 H, m), 1.78 – 2.09 (3 H, m), 2.22 – 2.31 (1 H, m), 2.36 – 2.45 (1 H, m), 2.52 (1 H, ddt,  $J$  9.8, 7.8, 4.9), 2.75 (1 H, dd,  $J$  13.6, 10.0), 2.83 (2 H, t,  $J$  7.6), 3.08 (2 H, t,  $J$  7.5), 3.19 (1 H, m), 3.63 (2 H, t,  $J$  7.5), 6.68 (1 H, s), 6.97 (1 H, s), 7.03 (1 H, d,  $J$  8.0), 7.23 (1 H, d,  $J$  8.0), 7.35 – 7.46 (2 H, m), 7.48 (1 H, s), 7.81 (1 H, dt,  $J$  7.2, 1.5), 7.86 (1 H, s).  $^{13}\text{C}$  NMR  $\delta_{\text{C}}$  (acetone- $d_6$ ): 14.1, 26.4, 27.4, 28.5, 30.0, 32.9, 34.2, 38.0, 38.5, 39.5, 45.3, 49.0, 49.6, 51.6, 126.2, 126.2, 126.9, 128.9, 129.1, 130.0, 132.8, 135.4, 137.2, 137.3, 139.1, 141.4, 168.9, 221.1. LR-MS for  $\text{C}_{28}\text{H}_{33}\text{O}_2\text{NBr}$   $[\text{M} + \text{H}]^+$ : 494.2 ( $^{79}\text{Br}$ ) and 496.2 ( $^{81}\text{Br}$ )  $m/z$ . HPLC purity of 95.6 % (retention time = 18.7 min).

#### 2.1.4. $^3\text{H}$ -PBRM

To a solution of PBRM-O (10 mg, 0.02 mmol) in MeOH (3 mL) was added  $\text{NaBT}_4$  (50  $\mu\text{L}$ , 2 mCi) at room temperature and under an argon atmosphere. The solution was stirred for 1 h and then  $\text{NaBH}_4$  (4 mg, 0.1 mmol) was added and the reaction monitored by TLC until completion. The resulting solution was poured into water (75 mL) and extracted with EtOAc (15 mL). The organic phase was dried over  $\text{Na}_2\text{SO}_4$ , filtered, and evaporated under reduced pressure. The residue was characterized by TLC (DCM/MeOH; 95:5) as a single spot corresponding to PBRM (same retention time for both tritiated ( $^3\text{H}$ ) and untritiated PBRM). The mixture of PBRM and  $^3\text{H}$ -PBRM was conserved in EtOH (150  $\mu\text{L}$ ) at  $-20\text{ }^\circ\text{C}$  and used as such in the experiments. A specific activity of 19.2 mCi/mmol was measured, giving a radiochemical yield of 76%.

## 2.2. *In vitro* studies

### 2.2.1. Stability of PBRM in human liver microsomes

The experiments were performed in a phosphate buffer (0.05 M, pH 7.5) containing PBRM (50  $\mu\text{M}$ ), a mixture of  $^3\text{H}$ -PBRM/PBRM (5/45  $\mu\text{M}$ ),  $^3\text{H}$ -PBRM (10  $\mu\text{M}$ ) or  $^3\text{H}$ -PBRM (1  $\mu\text{M}$ ) and incubated on a stirring plate at  $37\text{ }^\circ\text{C}$  with human liver microsomes (250  $\mu\text{g}$  of UltraPool (mix) HLM 150, 20 mg of protein / mL) from Corning Life Sciences (Tewksbury, MA, USA). The reaction was started by the addition of cofactor NADH (10 mM) in a final incubation volume of 250  $\mu\text{L}$ .

For the experiment with only PBRM (50  $\mu$ M): After incubation (2, 4, 8, 12 and 24 h), the reaction was stopped by the addition of purified water (250  $\mu$ L) and an aqueous 1 mM solution of ammonium acetate (500  $\mu$ L). An internal standard (compound RM-132 in reference [20]) was added, and after stirring, the solution was centrifuged (4000 g, 10 min at 4 °C). The supernatant was slowly deposited on two Strata-X SPE cartridges (Phenomenex, Torrance, CA, USA) preconditioned with MeOH (2 mL) and water (2 mL). A slow elution was performed followed by a washing using a MeOH/water (10:90) solution (2 mL). Finally, PBRM and its potential metabolites were eluted with a 5 mM solution of ammonium acetate in MeOH. This organic phase, which contains PBRM, was evaporated under a nitrogen stream. Both residues from the two cartridges of the same reaction were combined with MeOH and then evaporated under a nitrogen stream. The final residue was reconstituted with a MeOH/water (85:15) solution (200  $\mu$ L) and transferred into a glass insert. A portion (60  $\mu$ L) of this mixture was injected for LC-MS analysis (Shimadzu LCMS-2020, APCI, Alltima HP C18 column (250 mm x 4.6 mm, 5  $\mu$ m)). The solvent gradient started with a mixture of MeOH/water (70:30) and finished with MeOH (100%) over 40 min at a flow rate of 1 mL/min. The wavelength of the UV detector was selected at 195 nm.

For the experiment with  $^3$ H-PBRM: After incubation (0.5, 1, 2 and 4 h), the reaction mixtures were treated as reported above, but metabolite profiles were analyzed by LC system using a Luna C18 column (150 x 3 mm, 3 $\mu$ m; Phenomenex, Torrance, CA, USA) at a flow rate of 0.3 mL/min. Compound detection was performed with a Radiomatic 500TR flow scintillation detector (Packard, Meriden, CT, USA) and with an API 4000 mass spectrometer equipped with TurboIonSpray (Applied Biosystems) and ESI in negative ion mode. Radioactive peaks in the chromatogram were also assigned to chemical structures by matching them with co-chromatographed authentic standard and quantified by integrating peak areas.

### 2.2.2. Stability of PBRM in cells expressing 17 $\beta$ -HSD2

ZR-75-1 cells naturally expressing 17 $\beta$ -HSD2 [21] and HEK-293 cells overexpressing 17 $\beta$ -HSD2 (HEK-293[17 $\beta$ -HSD2]) [22] were maintained at 37 °C under 5% CO<sub>2</sub> humidified atmosphere. For ZR-75-1 cells, they were grown in RPMI-1640 medium supplemented with 10% fetal bovine serum (FBS), 1% penicillin/streptomycin and 2 mM L-glutamine. For HEK-



293[17 $\beta$ -HSD2] cells, they were grown in MEM medium supplemented with 10% FBS, 1% penicillin/streptomycin, 2 mM L-glutamine, 4.5 g/L D-glucose, 10 mM HEPES, 1 mM sodium pyruvate and 250  $\mu$ g/mL hygromycin. Cells were plated in 24-well culture at 50,000 cells per well. After incubation for 24 h,  $^3$ H-PBRM or  $^3$ H-E2 (American Radiolabeled Chemicals Inc.; St. Louis, MO, USA) were added into each well. At the desired incubation times, the culture medium was collected in tubes, the cells were trypsinated (with trypsin) and recovered in the test tubes containing cell supernatant, and the wells rinsed with super-Q water (500  $\mu$ L). The tubes combining both the supernatant and cells were treated by 5 cycles of sonication (30 sec), with a 30-sec pause between each cycle. Steroids were then extracted two times with diethyl ether, the combined organic phase washed with super-Q water and the steroids separated by TLC using two different eluent systems: toluene/acetone (4:1) for E2 and E1 and acetone only for PBRM and PBRM-O. Once the TLC plates were dry, the migration of PBRM and E2 were identified under UV irradiation and the spot corresponding to each steroid was cut. The piece of silica plate was added to Biodegradable Counting Scintillant (BCS, Amersham Biosciences, Piscataway, NJ, USA), vigorously stirred and incubated overnight at room temperature. The next day, radioactivity was evaluated using a Wallac 1411 liquid scintillation counter (Perkin Elmer, Woodbridge, ON, Canada).

### 2.2.3. Stability of PBRM in human plasma

Human blood was collected from different donors into collection heparin-coated tubes (Becton Dickinson, Franklin Lakes, NJ, USA). Blood was centrifuged at 2,200  $g$  for 20 min at 4  $^{\circ}$ C, the resulting plasma aliquoted into 10 mL volumes and stored at -80  $^{\circ}$ C. For the assay, human plasma was thawed and pre-warmed on a thermoregulated agitation plate, at 60 oscillations/min and 37  $^{\circ}$ C. A solution of PBRM dissolved in DMSO (6  $\mu$ L of 500  $\mu$ M) was added to 594  $\mu$ L of plasma, in duplicates. After 2, 4 and 6 h, samples (100  $\mu$ L) were quenched on ice with a solution of acetonitrile (300  $\mu$ L) containing an internal standard (RM-132 described in reference [20]). They were stored at -80  $^{\circ}$ C for 30 min to aid protein precipitation prior to centrifugation at 2,200  $g$  for 20 min. Supernatants (240  $\mu$ L) were collected and diluted with equal volume of super-Q water. Samples were then filtered and 60  $\mu$ L were assessed by LC-MS (Shimadzu LCMS-2020, APCI, Alltima HP C18 column (250 mm x 4.6 mm, 5  $\mu$ m)). Separation

was achieved with a gradient of MeOH:water (70:30) to MeOH (100%) at a flow rate of 0.8 mL/min over 40 min. The wavelength of the UV detector was selected at 195 nm.

#### 2.2.4. 17 $\beta$ -HSD1 inhibitory activity of PBRM-O

A comparative 17 $\beta$ -HSD1 inhibition assay between PBRM and its oxidized metabolite PBRM-O was realized at three concentrations (0.1, 1.0 and 10.0  $\mu$ M) in T-47D cells (5000 cells). Following a well-known protocol [8], T-47D cells were pre-incubated at 37 °C with the inhibitor for 0.5 h, the substrate <sup>14</sup>C-E1 (60 nM) (American Radiolabeled Chemicals Inc., St. Louis, MO, USA) was then added and the solution incubated at 37 °C. After 15 h, steroids (<sup>14</sup>C-E2 and <sup>14</sup>C-E1) were extracted with diethyl, dropped on TLC plates, eluted with toluene/acetone (4:1) and the radioactivity associated with each steroid was quantified using a Storm 860 Molecular Imager system (Molecular Dynamics, Sunnyvale, CA, USA).

#### 2.2.5. Estrogenic activity of PBRM-O

The proliferation of estrogen-sensitive T-47D cells was assessed to determine the potential *in vitro* estrogenic activity of PBRM-O. Following a well-known protocol [23], cells were treated 7 days in the presence of PBRM-O, PBRM or E2 (used as a positive control) and cell proliferation was monitored by the MTS method.

### 2.3. *In vivo* studies

#### 2.3.1. Animals

All animal experiments were conducted in an animal facility approved by the Canadian Council on Animal Care (CCAC) and the Association for Assessment and Accreditation of Laboratory Animal Care, and protocols were approved by the institutional animal ethics committee (Université Laval, Québec, Canada). All animals (mice and rats) were acclimatized to the environmental conditions (temperature, 22  $\pm$  3 °C; humidity, 50  $\pm$  20%; 12-h light/dark cycles, lights on at 07:15 h) for at least 3 days before starting the experiments. BALB/c female mice weighing approximately 20 g and Sprague-Dawley male rats (CrI:CD(SD)Br VAF/Plus) weighing approximately 220 g were obtained from Charles River, Inc. (Saint-Constant, QC, Canada). They were housed 3 per cage for mice and 3 to 5 per cage for rats. The animals were

allowed free access to water and food (Rodent Diet #T.2018.15, Harlan Teklad, Madison, WI, USA).

### 2.3.2. Measurement of PBRM, PBRM-O and $^3\text{H}$ -PBRM in animal tissues

Concentrations of PBRM and PBRM-O in blood samples were determined using a procedure developed at CHU de Québec - Research Center for steroid derivatives [7, 24].  $^3\text{H}$ -PBRM was quantified by liquid scintillation using 10 mL of BCS scintillation cocktail (GE Healthcare Lifesciences, Mississauga, ON, Canada) added to each polypropylene vial. Radioactivity was measured using a Wallac 1411 liquid scintillation counter (Perkin Elmer, Woodbridge, ON, Canada).

### 2.3.3. Plasmatic concentration of PBRM and PBRM-O in mice

Female mice received a single dose of PBRM (14.7 mg/kg in 0.1 mL of vehicle fluid) by subcutaneous (*sc*) injection or oral gavage (*po*). Depending on the vehicle used, the PBRM was first dissolved in EtOH or DMSO and, thereafter, we added the appropriate co-solvent (propylene glycol (PG), sunflower oil (SO) or 0.4% aqueous methylcellulose (MC)) to obtain a final 8% concentration of EtOH or DMSO. During this experiment, mice were fasted with free access to water for 8 h before the injection of PBRM. At the appropriate time point, 7 h (or 5 and 7 h) for those receiving DMSO as co-solvent and 6-time points (3, 5, 7, 9, 12 and 24 h) for those receiving EtOH as co-solvent, mice (2-3 per group) were sacrificed under isoflurane by cardiac puncture followed by cervical dislocation. Blood from each group was collected into Microvette potassium-EDTA (ethylenediamine tetraacetic acid)-coated tube (Sarstedt, AG & Co., Nümbrecht, Germany) and centrifuged at 3,200 rpm for 10 min at 4 °C. The plasma was collected and stored at -80 °C until the concentration of PBRM was determined by LC-MS/MS analysis as reported in section 2.3.2 [7, 24]. The concentration of PBRM-O was also determined by LC-MS/MS, but only for plasma samples collected from the experiment using PG/EtOH injected *sc*.

### 2.3.4. Determination of PBRM pharmacokinetic parameters

A single dose of PBRM was administered to female mice (2-3 animals/time-point per dose) using the following two vehicles: 1) PG/DMA(dimethylacetamide)/DMSO (60:38:2)

(intravenous (*iv*), PBRM at 2 mg/kg) and 2) MC/DMSO (92:8) (*sc*, PBRM at 14.7 mg/kg). Blood was collected by cardiac puncture at various time points of 0.08, 0.5, 1, 2, 3, 4, 5, 6 and 7 h post-dose for *iv* and 0.25, 0.5, 1, 2, 3, 4, 5, 6, 7 and 12 h post-dose for *sc*, pooled for each group, the plasma obtained as described above and the levels of PBRM measured as reported above. Plasma concentrations at the same endpoint were averaged and non-compartmental analysis was performed to the averaged blood concentration vs time curve. Pharmacokinetic parameters were calculated using Phoenix WNL version 5.1 (Princeton, NJ, USA) and the following formula was used for bioavailability determination:  $F = AUC_{(0-\infty) sc} \times Dose_{iv} / AUC_{(0-\infty) iv} \times Dose_{sc}$ .

### 2.3.5. Plasma concentration of <sup>3</sup>H-PBRM in mice and rats

Female mice and male rats received a single *sc* injection of a mixture of <sup>3</sup>H-PBRM/PBRM (0.3/99.7%) at a dose of 14.7 mg/kg in 0.1 or 1.5 mL of vehicle fluid, respectively. The inhibitor was first dissolved in DMSO, and MC was added to obtain a final 8% concentration of co-solvent. For the mice, blood was collected by cardiac puncture from 2 animals per time point (0.25, 0.5, 1, 2, 3, 4, 5, 6, 7 and 12 h). For the rats, blood samples were collected at the jugular vein (0.4 mL by animal) from 3 animals per time point (0.25, 1, 2, 3, 4, 5, 6, 7 and 12 h). After the collection at 7 h, a replacement fluid (0.9% sodium chloride USP) was injected in each rat. Blood from each group was pooled, the plasma collected as described above and the radioactivity was quantified, as reported above.

### 2.3.6. Biodistribution of PBRM in mice

<sup>3</sup>H-PBRM (14  $\mu$ Ci/100  $\mu$ g) in a solution of 100  $\mu$ L PG/EtOH (92:8) was administered by *sc* injection to three female mice. Animals were sacrificed 3, 6, 12, 24, 48 and 72 h after administration. Blood was preserved into Microvette potassium-EDTA-coated tubes (Sarstedt, AG & Co.) and thereafter centrifuged at 3,200 rpm for 10 min at 4 °C. Other tissues were then collected and dissolved with KOH (10 N), as well as the remaining carcass. Samples (100  $\mu$ L) of dissolved tissues were bleached with 30% H<sub>2</sub>O<sub>2</sub> (50  $\mu$ L) for 1 h at 37 °C in scintillation vials. Each vial was then aerated and radioactivity was measured as reported above by liquid scintillation 48 h later once the chemiluminescence caused by KOH was reduced to background level.

### 2.3.7. Mass balance of PBRM in mice

Two female mice were housed individually in metabolic cages. After at least 48 h of acclimatization, a dose of  $^3\text{H}$ -PBRM (10  $\mu\text{Ci}/72 \mu\text{g}$ ) in PG/EtOH/saline (46:8:46) was injected *iv* in the caudal vein. The animals stayed in the metabolic cages for one week, during which urine and feces were collected at different times (0.5, 1, 2, 3, 4, 5, 6 and 7 days). After each collection, the cage was thoroughly and successively washed with EtOH and water. Samples of urine and wash liquid were counted directly by liquid scintillation, as described above. Feces were beforehand diluted and bleached in a sodium hypochlorite 3% solution. Mice were also sacrificed and their tissue collected, dissolved and remaining radioactivity quantified as done for the biodistribution experiment.

### 2.3.8. Maximum tolerated dose and dose accumulation in mice

First part (maximum tolerated dose): We determined the limit dose of PBRM tolerated by female mice, i.e. the maximum dose which does not cause toxic effects in animals (weight loss below 20%, inability to eat or to drink, abnormal posture, movement, or vocalization). It is important to note that animal death is not an accepted endpoint for CCAC. On the starting day, PBRM was administered by *sc* injection or *po* (gavage needle). PBRM was first dissolved in DMSO and MC or SO was added to obtain a final 8% concentration of co-solvent. The injected volume was 0.1, 0.25, 0.35 or 0.5 mL (*sc*) and 0.5 mL (*po*), but the number of injections ranged from 1, 2 or 3 to obtain the expected dose. After the administration of PBRM, the mice were observed and weighed for 7 days to notice any signs of toxicity. The protocol was applied to four groups, 8 mice per group, divided as follow: Group 1: vehicle administrated weekly by *sc* injection of MC/DMSO (92:8) for 8 consecutive weeks; Group 2: vehicle administrated weekly by *po* injection of SO/DMSO (92:8) for 5 consecutive weeks; Group 3: PBRM administrated weekly by *sc* injection (30, 45, 60, 90, 135, 180, 270 and 405 mg/kg) for 8 consecutive weeks; Group 4: PBRM administrated weekly by *po* injection (300, 450, 600, 900 and 1350 mg/kg) for 5 consecutive weeks.

Second part (dose accumulation): At the end of the first part, the residual healthy female mice were observed for an additional week to allow a complete elimination of PBRM. After that, the mice were randomized and used for the second part of the protocol, which consisted in

evaluating the effect of repeated administration of a dose of PBRM (*sc* or *po*). The vehicles used for this experiment were the same as the ones previously used in the first part of the protocol. The mice were divided into four groups as follow: Group 1: vehicle (0.1 mL) administered daily for 4 days by *sc* injection of MC/DMSO (92:8) into 2 mice; Group 2: vehicle (0.5 mL) administered daily for 4 days by *po* injection of SO/DMSO (92:8) into 2 mice; Group 3: PBRM (0.1 mL) administered daily by *sc* injection (45 mg/kg) during 1 (2 mice), 2 (2 mice), 3 (2 mice) and 4 days (4 mice); Group 4: PBRM (0.5 mL) administered daily by *po* injection (450 mg/kg) during 1 (2 mice), 2 (2 mice), 3 (2 mice), and 4 days (4 mice). During the protocol, the mice were observed and weighed each day. Blood was also collected 3 h post-injection following 2, 3 and 4 days of treatment, the plasma obtained and the concentration of PBRM measured each day, as reported above.

### 3. Results

#### 3.1. *In vitro* studies with PBRM

##### 3.1.1. Stability in human liver microsomes

The study of PBRM in human liver microsomes is a useful predictive tool to evaluate its stability, as well as the potential metabolites. After incubation (0-4 h) of <sup>3</sup>H-PBRM/PBRM (1, 10 and 50  $\mu$ M) in microsomes using NADH as a cofactor, we observed a gradual disappearance of PBRM coupled with a gradual appearance of the corresponding oxidized form of PBRM at position C17 (Fig. 2A-C). The PBRM-O metabolite identification was confirmed by an injection of the synthetic PBRM-O as standard, which matched perfectly with the LC-MS retention time and mass spectrum from the metabolism experiment (Supplementary Material, Fig. S1). A second experiment (0-24 h) using PBRM in human microsomes and NADH also confirmed that no other metabolite was formed at another position in the molecule (Fig. 2D). Indeed, the disappearance of PBRM, due to its oxidation at position C17 to a ketone (PBRM-O) by microsomal CYPs, was the only metabolite of phase-I observed during this 24 h assay.

##### 3.1.2. Stability of PBRM over oxidative 17 $\beta$ -HSD2

Since the alcohol ( $17\beta$ -OH) functionality of PBRM was subject to oxidative enzymes, as observed in liver microsomes, we were curious to see if this oxidation could occur in breast cancer cells via the  $17\beta$ -HSD2. This steroidogenic enzyme is well-recognized to oxidize the  $17\beta$ -hydroxyl of E2 into the 17-carbonyl of E1 [12]. We thus evaluated the stability of  $^3\text{H}$ -PBRM in ZR-75-1 cells, which naturally express  $17\beta$ -HSD2 and other oxidative  $17\beta$ -HSDs (types 4 and 8) [21], as well as in HEK-293 cells transfected with  $17\beta$ -HSD2 [22]. We did not observe any significant reduction of  $^3\text{H}$ -PBRM level ( $17\beta$ -OH oxidation) after 72 h of incubation in both cell lines (Fig. 3A).  $^3\text{H}$ -E2 was used as a positive control in the assay and we observed, as expected, a medium to high decrease of E2 ( $17\beta$ -OH oxidation) depending on the cell line (Fig. 3B).

### 3.1.3. Stability in human plasma

We incubated PBRM in human plasma at  $37^\circ\text{C}$ . After 2, 4 and 6 h, the inhibitor PBRM was quantified by LC-MS and the values reported as the % of remaining inhibitor vs the initial quantity incubated. In this experiment, PBRM was fully stable during the period studied (Fig. 4).

### 3.1.4. $17\beta$ -HSD1 inhibition and estrogenic activity of PBRM-O metabolite

As the sole metabolite observed so far, the  $17\beta$ -HSD1 inhibitory activity and estrogenic activity of PBRM-O were tested in T-47D breast cancer cells (Table 1). This cell line expresses both  $17\beta$ -HSD1 and the estrogen receptor [25]. PBRM-O showed good inhibition of the transformation of  $^{14}\text{C}$ -E1 into  $^{14}\text{C}$ -E2 in T-47D cells (49 and 87% at 0.1 and  $1\ \mu\text{M}$ , respectively). In fact, we only measured a slight loss of potency compared to PBRM (71 and 95% at 0.1 and  $1\ \mu\text{M}$ , respectively). When tested on estrogen-sensitive T-47D cells, PBRM-O did not stimulate cell proliferation at 0.1 and  $1\ \mu\text{M}$ , suggesting a non-estrogenic compound.

## 3.2. *In vivo* studies of PBRM

### 3.2.1. Stability in mice

We treated mice with a single *sc* injection of PBRM ( $250\ \mu\text{g}$  in PG/EtOH (92:8);  $14.7\ \text{mg/kg}$ ) and measured the plasma concentration of PBRM and PBRM-O at different times (0, 3, 5, 7, 9, 12 and 24 h) (Fig. 5). Interestingly and contrary to the *in vitro* assay, the formation of PBRM-O represented only a small fraction of the PBRM in plasma ( $< 1\%$  of PBRM  $\text{AUC}_{(0-24\ \text{h})}$ ).

These results open the door to a biodistribution study using  $^3\text{H}$ -PBRM as stable radiolabeled compound.

### 3.2.2. Modes of administration and vehicles

PBRM is a hydrophobic steroid derivative ( $\text{CLog P} = 5.8$ ) having low solubility in water and, consequently, must be administered in an appropriate vehicle. Typically, PBRM is first dissolved in an organic solvent (EtOH or DMSO) before being mixed in MC, PG, or SO. As an initial step before the determination of pharmacokinetic parameters in mice, we investigated six vehicles to administrate PBRM *sc* or *po* at a dose of 14.7 mg/kg. We first administered three formulations with EtOH as organic solvent and measured the plasma concentration of PBRM obtained at 6 time points (3, 5, 7, 9, 12 and 24 h) as well as determined the  $\text{AUC}_{(0-7\text{h})}$  and  $\text{AUC}_{(0-24\text{h})}$  (Table 2).

For the *sc* mode, PG/EtOH (92:8) and SO/EtOH (92:8) gave similar values ( $\text{AUC}_{(0-24\text{h})} = 6,844$  and  $6,450$  ng.h/mL, respectively), which are slightly higher values than those obtained for MC/EtOH (92:8) ( $\text{AUC}_{(0-24\text{h})} = 4,244$  ng.h/mL). On the other hand, for the *po* mode, the best formulation was found for the SO/EtOH (92:8), with an  $\text{AUC}_{(0-24\text{h})}$  value of 3312 ng.h/mL. This vehicle provided a slightly higher value than MC/EtOH (3,137 ng.h/mL) and a value higher than PG/EtOH (2,776 ng.h/mL). Interestingly, the best  $\text{AUC}_{(0-24\text{h})}$  values obtained for the *po* mode correspond to approximately 50% of the best values found for *sc* mode.

We also verified the impact on the plasma concentration at a comparative time point (7 h) of changing the co-solvent EtOH to DMSO. Plasma concentration of PBRM injected *sc* in MC/DMSO, PG/DMSO and SO/DMSO was higher at 7 h than the concentration observed in MC/EtOH, PG/EtOH and SO/EtOH. However, for *po* administration, the plasma concentration of PBRM was roughly the same for DMSO, and EtOH as co-solvent. Thus, at the end of this study, MC/DMSO (92:8) was retained for *in vivo* assays (*sc* mode) aimed to determine the pharmacokinetic parameters.

### 3.2.3. Pharmacokinetic profile and parameters in mice

The pharmacokinetic parameters characterize the fate of a drug, and they are obtained from curves that represent the evolution of its plasma concentration for a given mode of



administration. After selecting MC/DMSO (92:8) and PG/DMA/DMSO (60:38:2) for the administration of PBRM in mice *sc* and *iv*, respectively, we generated curves with sufficient data for purposes of analysis (Supplementary Material, Fig. S2-S6). The parameters resulting from these curves are summarized in Table 3. Following intravenous (*iv*) administration of PBRM at 2 mg/kg, plasma concentrations declined with a half-life value of 2.2 h. Based on plasma data, total body clearance was estimated at 1,358 mL/h.kg (corresponding to 0.57 mL/min for a 25-g mouse). Assuming no distribution of the drug into the erythrocytes, the total body clearance is less than the cardiac output in mice (8 mL/min) and thus total body extraction (E organ) is estimated to be 0.07. Accordingly, PBRM has a low overall body extraction. The volume of distribution was estimated at 4,270 mL/kg following an administration of PBRM, thus exceeding the extracellular volume and showing a high extent of PBRM total body distribution. Following *sc* administration of PBRM in MC/DMSO (92:8) at a dose of 14.7 mg/kg, plasma concentration of PBRM peaked at 3 h post-dose. After reaching a  $C_{max}$  value of 990 ng/mL, the PBRM concentration readily declined with a half-life value of 3.4 h. The systemic exposure was evaluated at 7,042 ng.h/mL. Relative to the *iv* route of administration, the absolute bioavailability (F) was calculated to be 65% for *sc* administration. Using the  $AUC_{(0-24h)}$  value measured when PBRM was injected in SO/EtOH (92:8) at 14.7 mg/kg (Table 2), it is also possible to estimate a F value of 33% for *po* administration.

#### 3.2.4. Plasma concentration in mice vs rats

In a comparative experiment, we determined the plasma concentration of  $^3\text{H}$ -PBRM as a function of time following a *sc* administration in two rodent species (mice and rats). The two curves reported in Figure 6 follow the same tendency until 4 h, with roughly the same concentration of  $^3\text{H}$ -PBRM measured, but the curves differ, thereafter. In fact, the  $^3\text{H}$ -PBRM concentration decreased faster in mice than in rats, representing only 45% at 12 h.

#### 3.2.5. Biodistribution in mice

To further evaluate the pharmacokinetics of PBRM, the tissue distribution of the radiolabeled inhibitor was observed in mice after *sc* administration (Fig. 7). Most tissues appeared to reach maximal level of  $^3\text{H}$ -PBRM 6 h after injection. The radioactivity was mostly observed in the digestive tract for the first 6 h after injection. Mice sacrificed 12 h after injection

showed lower levels in the intestines and colon than those sacrificed after 6 or 24 h. This deviation could be explained by the fact that the administration of PBRM was done for the 12 h mice in the evening, while the other two were injected in the morning. Moreover, stomach, intestine and colon contents appear to have higher radioactivity levels than other tissues (Fig. 7). In fact, the intestine was the only organ where the presence of PBRM could still be detected after 3 days (Fig. 7A). This observation points out to a strong fecal excretion of PBRM and this 17 $\beta$ -HSD1 inhibitor did not appear to accumulate in any organ. In fact, PBRM was barely or non-detectable in most of tissues outside of the digestive tract (Fig. 7B). Overall, the lack of PBRM accumulation is reassuring in regards to safety concerns raised by a covalent mechanism of inhibition.

### 3.2.6. Excretion (mass balance) in mice

To have a better idea of PBRM excretion, a mass balance assay was conducted in mice. <sup>3</sup>H-PBRM was administered by *iv* injection to mice kept in metabolic cages. Feces and urine were collected regularly and cages were washed each time. Radioactivity was then quantified in feces, urine and wash liquid. The PBRM was mostly recovered in feces with 93%, against 7% in urine (Fig. 8). The radioactivity recovered in the washing liquid accounts for less than 0.5% of the injected radioactivity. The elimination occurred in the first 24 h (68%) and continued at a lower rate until 5 days after the injection, when it reached a plateau.

### 3.2.7. Maximum tolerated dose in mice

The maximum tolerated dose (MTD) was determined in mice for two different vehicles according to the mode of administration (MC/DMSO (92:8) and SO/DMSO (92:8) for *sc* and *po*, respectively) (Fig. 9). However, for *po* administration, we used DMSO instead of EtOH, as a co-solvent with MC, because the better solubility of this vehicle allowed us to achieve a higher limit of PBRM solubility. In the first part of the experiment, increasing doses of PBRM were given once a week, and animals were carefully monitored during the week for toxicity signs approved by our ethics committee. No sign of toxicity was noted for each dose of PBRM (30, 45, 60, 90, 135, 180, 270 and 405 mg/kg/week) given by *sc* injection for 8 consecutive weeks. In fact, the titration of the dose was limited by the solubility of PBRM in the volume of MC/DMSO (92:8) allowed for injection (0.1 to 1 mL). No sign of toxicity was observed, either, for the first 3 doses

(300, 450 and 600 mg/kg/week) of PBRM given orally by gavage (*po*) during 3 consecutive weeks. At the dose of 900 mg/kg (week 4), however, signs of toxicity such as diarrhea and fatigue appeared a few days after administration. These symptoms became more severe at the 1350 mg/kg dose. These signs were however also present in the control group of mice receiving no PBRM but only the vehicle (SO/DMSO (92:8)) in a volume ranging from 0.5 to 1 mL. After 5 weeks, 3 mice were dead in the treated groups, as well in the control group. Since these adverse effects were observed at high oral doses in both groups (treated and control), we concluded that the vehicle (SO/DMSO (92:8)) was in cause. In fact, at this higher dose, the total volume of SO received by the mice was 1 mL, representing an important volume of both oil and DMSO for a mouse of about 20 g. Consequently, the signs of toxicity observed for the *po* vehicle used, especially diarrhea, were associated with the high volume of the vehicle used, rather than the higher dose of PBRM.

In the second part of the MTD experiment, the *sc* injection of PBRM each day at 45 mg/kg in MC/DMSO (92:8) for 4 consecutive days showed no sign of toxicity and no anomaly at animal necropsy. Furthermore, the concentration of PBRM measured in plasma increased after the first injection, but peaked and stabilized between 2-4 days (Fig. 10). In the case of oral administration (*po*) by gavage at 450 mg/kg in SO/DMSO (92:8), no signs of toxicity were noted and no anomaly was observed in animals at necropsy. Similarly, as observed for the *sc* injection of PBRM, the *po* administration did not produce an accumulation of the inhibitor when administered each day. In fact, the plasma concentration reached a plateau after the first administration, suggesting a low risk of toxicity and potentially the result of enzyme induction.

#### 4. Discussion

This study focuses on PBRM behavior related to different and fundamental aspects of pharmacology, such as metabolism, pharmacokinetics, stability, and safety. *In vitro*, the assay performed in human hepatic microsomes raises interesting information about the stability of PBRM, as well as the metabolites formed from phase-I metabolism. A first important observation was the gradual oxidation of PBRM at position 17 to give the corresponding ketone as the sole phase-I metabolite observed, namely PBRM-O. Interestingly, PBRM-O did not show any *in vitro* estrogenic activity (proliferation of T-47D cells) and was found to be an active 17 $\beta$ -

HSD1 inhibitor with only a slight drop in activity compared to PBRM. This PBRM metabolite could thus extend the inhibition induced by PBRM. An interesting point was the formation of a single metabolite, which contrasts with the usual multiple metabolite profile of the estrane-based scaffold, such as E2 and its derivatives [26]. We hypothesized that the presence of a short bromoethyl side-chain a position 3, in replacement of the 3-OH, deactivates the steroid A-ring toward hydroxylation at other positions, thus resulting in a stabilization effect toward CYP enzymes.

*In vivo*, a very small proportion of PBRM-O representing less than 1% of PBRM plasma concentration was found during a 24-h period following *sc* injection. This result was very important because it allowed us to use a radiolabeled version of PBRM ( $^3\text{H}$ -PBRM) for pharmacokinetic and biodistribution studies without fear of losing the tritium ( $^3\text{H}$ ) atom due to its oxidation to PBRM-O. In fact, the tritium atom was introduced at C17 $\alpha$  of PBRM, a position that was found to be non-reactive, considering the bulky environment provided by the C18-methyl and C16 $\beta$ -benzylamide side-chain. The 17 $\beta$ -alcohol is thus protected from a potential oxidation, glucuronidation, or sulfatation reaction.

We assessed the pharmacokinetic parameters of this first steroidal covalent non-estrogenic inhibitor of 17 $\beta$ -HSD1 (PBRM) and obtained favorable values regarding half-life ( $T_{1/2}$ ), absolute bioavailability (F), distribution volume ( $V_z$ ) and clearance rate (CL). For example, the  $C_{\text{max}}$  (990 ng/mL) of PBRM in mice represents a concentration reaching 2  $\mu\text{M}$ , which is more than 10 times higher to the  $\text{IC}_{50}$  value (68 nM) initially obtained in the 17 $\beta$ -HSD1 cell inhibition assay. This concentration seems largely sufficient to exert its inhibitory action during the main part of a 24-h period. These favorable pharmacokinetic data are in agreement with the successful *in vivo* proof-of-principle previously reported, which showed a complete blockade of E1-induced tumor progression in T-47D breast cancer xenografts at 14.7 mg/kg/day of PBRM injected *sc* in mice [7]. Furthermore, and importantly, this new pharmacokinetic study also revealed that PBRM was orally bioavailable (F = 33% relative to *iv* route of administration), which represents an advantage toward clinical development for a daily based therapy. Complementary to these results, a study with  $^3\text{H}$ -PBRM injected in two rodent species (mouse and rat) showed that the metabolism of PBRM is faster in mice than in rats, as expected [27, 28].

A distribution study using  $^3\text{H}$ -PBRM was realized to give an overview of the PBRM apportionment in different mouse tissues following *sc* administration. As a first observation, no accumulation in any organ was noted after 72 h. Also, a peak of detection was found 6 h after PBRM injection, occurring as expected principally in the liver, kidney and gastrointestinal tract [29]. This peak detection was followed by a gradual elimination of these organs, over time (12, 24 and 48 h) until complete disappearance at 72 h. To be noted, small or no detection of  $^3\text{H}$ -PBRM was observed in mammary glands, uterus or ovaries, which tissues express  $17\beta$ -HSD1. This result was expected, since PBRM was shown to be a very weak inhibitor of mouse  $17\beta$ -HSD1 orthologs, due to the absence of His-221, replaced by Gly-221 to which the PBRM can't bind covalently [16]. Overall, the distribution profile of  $^3\text{H}$ -PBRM is coherent with simple blood distribution and gastrointestinal excretion, which is favorable for a candidate drug.

A mass balance study often represents a standard experiment in the development of a new drug candidate. We therefore injected  $^3\text{H}$ -PBRM in mice in order to obtain essential information about mass balance and routes of excretion [30]. Interesting observations were derived from this experiment. First, the levels of PBRM found in the gastrointestinal tract were high, and radioactivity was still detected, three days after injection. These results are coherent with the excretion results, which appear to be mainly fecal (93% found in feces) against 7% in urine. Elimination occurs rather slowly, as about one third of the dose was still in the animals 24 h after injection and took about 4 days before everything came out. This slow fecal excretion may explain the high PBRM level found in the gastrointestinal tract for a long period of time. These results point out a slow metabolism of the inhibitor that correlates with the relatively long plasma half-life of PBRM. However, since a full metabolism study (phase-I and phase-II) has not yet been formally addressed *in vivo*, appropriate experiments should be conducted to highlight this point, as well as the oral availability of PBRM that was already observed in a preliminary test. Further distribution studies will also have to consider the effect of excretion. Twelve-hour time point mice were injected in the evening, while others were injected in the morning. The goal was to avoid nightly sacrifice, but this seemed to affect distribution, as lower quantities of less PBRM was found in the intestines and colon of these mice than in those sacrificed 6 and 24 h after injection. Differences between night and day were also observed in the production of feces, but concentrations didn't seem to be significantly affected by the time of day chosen for injection.

PBRM was well-tolerated by mice in both the *sc* and *po* modes of administration. In *sc* mode, the limit of PBRM solubility was reached (405 mg/kg) in the MC/DMSO (92:8) vehicle used, without any signs of toxicity in acute or extended time-toxicity studies. In *po* mode, some signs of toxicity were observed before reaching the limit of PBRM solubility (1,350 mg/kg) in the vehicle (SO/DMSO, 92:8), but this toxicity was likely caused by the quantity of vehicle used. These *in vivo* results add to previous *in vitro* results that shown a weak affinity of PBRM when tested on a large panel of potential off-targets [16]. The favorable safety profile of PBRM, even at high doses, should provide an advantageous flexible therapeutic window regarding future efficiency dose optimization studies for either life-threatening diseases such as breast and endometrial cancers, or other chronic diseases, for example, endometriosis.

## 5. Conclusion

The steroidal  $17\beta$ -HSD1 covalent inhibitor PBRM presents a favorable pharmacological profile. Indeed, the measured pharmacokinetic parameters ( $C_{max}$ , AUC,  $T_{1/2}$ ,  $V_z$ , CL and F) are very acceptable, doubled by the fact that good oral bioavailability was observed. *In vitro* assays in hepatic microsomes show a gradual transformation of PBRM into one major metabolite corresponding to the oxidized 17-ketone form of PBRM, PBRM-O, which is also an inhibitor of  $17\beta$ -HSD1 that is devoid of estrogenic activity. However, the formation of PBRM-O represented only a very small proportion ( $< 1\%$ ) of PBRM *in vivo*, opening the doors to a tritium radiolabeling at position  $17\alpha$  of PBRM. The subsequent distribution study using PBRM showed no accumulation in the tissues, and excretion took days. This long staying time of PBRM is favorable for its efficiency as a time-dependent irreversible inhibitor. PBRM was also well-tolerated in mice at high concentration levels for a period of several weeks. Overall, these results highlight the potential of PBRM to be a new emerging drug that could reach clinical assays in the near future.

## Acknowledgments

We are thankful to Marie-Claude Trottier for NMR and LC-MS analyses, to Dr. Jean Gosselin who provided blood samples, and to Micheline Harvey for careful reading of this manuscript.

### **Conflict of interest**

The authors RM, JR and DP are inventors of a patent application related to 17 $\beta$ -HSD inhibitors. Other authors have no conflicts of interest.

### **Funding**

This research was supported by the Canadian Institutes of Health Research (CIHR) and by Amorchem Holding Funds (Montréal, QC, Canada).

### **Appendix A**

Supplementary material: 1) Identification of PBRM-O as a metabolite of PBRM (Figure S1) and 2) Curves used for the calculation of pharmacokinetic parameters (Figures S2-S6).

## References

- [1] T.A. Baillie, Targeted covalent inhibitors for drug design, *Angewandte chemie*, international edition, 55 (2016) 13408-13421.
- [2] A.S. Kalgutkar, D.K. Dalvie, Drug discovery for a new generation of covalent drugs, *Expert opinion on drug discovery*, 7 (2012) 561-581.
- [3] C. Gonzalez-Bello, Designing irreversible inhibitors-worth the effort?, *ChemMedChem*, 11 (2016) 22-30.
- [4] J. Singh, R.C. Petter, T.A. Baillie, A. Whitty, The resurgence of covalent drugs, *Nature reviews drug discovery*, 10 (2011) 307-317.
- [5] R. Mah, J.R. Thomas, C.M. Shafer, Drug discovery considerations in the development of covalent inhibitors, *Bioorganic and medicinal chemistry letters*, 24 (2014) 33-39.
- [6] R. Maltais, D. Ayan, D. Poirier, Crucial role of 3-bromoethyl in removing the estrogenic activity of 17 $\beta$ -HSD1 inhibitor 16 $\beta$ -(*m*-carbamoylbenzyl)estradiol, *ACS medicinal chemistry letters*, 2 (2011) 678-681.
- [7] D. Ayan, R. Maltais, J. Roy, D. Poirier, A new nonestrogenic steroidal inhibitor of 17 $\beta$ -hydroxysteroid dehydrogenase type I blocks the estrogen-dependent breast cancer tumor growth induced by estrone, *Molecular cancer therapeutics*, 11 (2012) 2096-2104.
- [8] R. Maltais, D. Ayan, A. Trottier, Discovery of a non-estrogenic irreversible inhibitor of 17 $\beta$ -hydroxysteroid dehydrogenase type 1 from 3-substituted-16 $\beta$ -(*m*-carbamoylbenzyl)-estradiol derivatives, *Journal of medicinal chemistry*, 57 (2014) 204-222.
- [9] E. Hilborn, O. Stål, A. Jansson, Estrogen and androgen-converting enzymes 17 $\beta$ -hydroxysteroid dehydrogenase and their involvement in cancer: with a special focus on 17 $\beta$ -hydroxysteroid dehydrogenase type 1, 2, and breast cancer, *Oncotarget*, 8 (2017) 30552-30562.
- [10] J.M. Day, H.J. Tutill, A. Purohit, M.J. Reed, Design and validation of specific inhibitors of 17beta-hydroxysteroid dehydrogenases for therapeutic application in breast and prostate cancer, and in endometriosis, *Endocrine-related cancer*, 15 (2008) 665-692.
- [11] S.X. Lin, D. Poirier, J. Adamski, A challenge for medicinal chemistry by the 17 $\beta$ -hydroxysteroid dehydrogenase superfamily: an integrated biological function and inhibition study, *Current topics in medicinal chemistry*, 13 (2013) 1164-1171.
- [12] D. Poirier, 17beta-Hydroxysteroid dehydrogenase inhibitors: a patent review, *Expert opinion on therapeutic patents*, 20 (2010) 1123-1145.
- [13] S. Marchais-Oberwinkler, C. Henn, G. Moller, T. Klein, M. Negri, A. Oster, A. Spadaro, R. Werth, M. Wetzel, K. Xu, M. Frotscher, R.W. Hartmann, J. Adamski, 17beta-Hydroxysteroid dehydrogenases (17beta-HSDs) as therapeutic targets: protein structures, functions, and recent progress in inhibitor development, *The journal of steroid biochemistry and molecular biology*, 125 (2011) 66-82.
- [14] K.M. Cornel, R.F. Kruitwagen, B. Delvoux, L. Visconti, K.K. Van de Vijver, J.M. Day, T. Van Gorp, R.J. Hermans, G.A. Dunselman, A. Romano, Overexpression of 17beta-hydroxysteroid dehydrogenase type 1 increases the exposure of endometrial cancer to 17beta-estradiol, *The journal of clinical endocrinology and metabolism*, 97 (2012) E591-601.
- [15] T.L. Rizner, Estrogen biosynthesis, phase I and phase II metabolism, and action in endometrial cancer, *Molecular and cellular endocrinology*, 381 (2013) 124-139.
- [16] A. Trottier, R. Maltais, D. Ayan, X. Barbeau, J. Roy, R. Poulin, P. Lagüe, M. Perreault, D. Poirier, Insight into the mode of action and selectivity of PBRM, a covalent steroidal inhibitor of 17 $\beta$ -hydroxysteroid dehydrogenase type 1, *Biochemical pharmacology*, 144 (2017) 149-161.



- [17] T. Kobayashi, C. Hoppmann, B. Yang, L. Wang, Using protein-confined proximity to determine chemical reactivity, *Journal of the American Chemical Society*, 138 (2016) 14832-14835.
- [18] M. Mazumdar, D. Fournier, D.-W. Zhu, C. Cadot, D. Poirier, S.-X. Lin, Binary and ternary crystal structure analyses of a novel inhibitor with 17 $\beta$ -HSD type 1: a lead compound for breast cancer therapy, *The Biochemical Journal*, 424 (2009) 357-366.
- [19] P. Greaves, A. Williams, M. Eve, First dose of potential new medicines to humans: how animals help, *Nature Reviews Drug Discovery*, 3 (2004) 226-236.
- [20] D. Ayan, R. Maltais, A. Hospital, D. Poirier, Chemical synthesis, cytotoxicity, selectivity and bioavailability of 5 $\alpha$ -androstane-3 $\alpha$ ,17 $\beta$ -diol derivatives, *Bioorganic and Medicinal Chemistry*, 22 (2014) 5847-5859.
- [21] Z.J. Liu, W.J. Lee, B.T. Zhu, Selective insensitivity of ZR-75-1 human breast cancer cells to 2-methoxyestradiol: evidence for type II 17 $\beta$ -hydroxysteroid dehydrogenase as the underlying cause, *Cancer Research*, 65 (2005) 5802-5811.
- [22] P. Bydal, S. Auger, D. Poirier, Inhibition of type 2 17 $\beta$ -hydroxysteroid dehydrogenase by estradiol derivatives bearing a lactone on the D-ring: structure-activity relationships, *Steroids*, 69 (2004) 325-342.
- [23] R. Maltais, A. Trottier, X. Barbeau, P. Lague, M. Perreault, J.F. Theriault, S.X. Lin, D. Poirier, Impact of structural modifications at positions 13, 16 and 17 of 16 $\beta$ -(*m*-carbamoylbenzyl)-estradiol on 17 $\beta$ -hydroxysteroid dehydrogenase type 1 inhibition and estrogenic activity, *The Journal of Steroid Biochemistry and Molecular Biology*, 161 (2016) 24-35.
- [24] F. Labrie, A. Belanger, P. Belanger, R. Berube, C. Martel, L. Cusan, J. Gomez, B. Candas, I. Castiel, V. Chaussade, C. Deloche, J. Leclaire, Androgen glucuronides, instead of testosterone, as the new markers of androgenic activity in women, *The Journal of Steroid Biochemistry and Molecular Biology*, 99 (2006) 182-188.
- [25] Y. Laplante, C. Rancourt, D. Poirier, Relative involvement of three 17 $\beta$ -hydroxysteroid dehydrogenases (types 1, 7 and 12) in the formation of estradiol in various breast cancer cell lines using selective inhibitors, *Molecular and Cellular Endocrinology*, 301 (2009) 146-153.
- [26] Y. Tsuchiya, M. Nakajima, T. Yokoi, Cytochrome P450-mediated metabolism of estrogens and its regulation in human, *Cancer Letters*, 227 (2005) 115-124.
- [27] M. Martignoni, G.M. Groothuis, R. de Kanter, Species differences between mouse, rat, dog, monkey and human CYP-mediated drug metabolism, inhibition and induction, *Expert Opinion on Drug Metabolism and Toxicology*, 2 (2006) 875-894.
- [28] M.A. Holliday, D. Potter, A. Jarrah, S. Bearg, The relation of metabolic rate to body weight and organ size, *Pediatric Research*, 1 (1967) 185-195.
- [29] U. Klotz, Pathophysiological and disease-induced changes in drug distribution volume: pharmacokinetic implications, *Clinical Pharmacokinetics*, 1 (1976) 204-218.
- [30] S.J. Roffey, R.S. Obach, J.I. Gedge, D.A. Smith, What is the objective of the mass balance study? A retrospective analysis of data in animal and human excretion studies employing radiolabeled drugs, *Drug Metabolism Reviews*, 39 (2007) 17-43.

## Tables and Figures

**Table 1.** 17 $\beta$ -HSD1 inhibitory activity and estrogenic activity of PBRM-O

ID	Inhibition (%) <sup>1</sup> at 0.1 $\mu$ M	Inhibition (%) <sup>1</sup> at 1 $\mu$ M	Inhibition (IC <sub>50</sub> ) <sup>1</sup> in $\mu$ M	Estrogenicity <sup>2</sup> at 0.1 and 1 $\mu$ M
PBRM	71 $\pm$ 2	95 $\pm$ 5	0.068 <sup>3</sup>	No
PBRM-O	49 $\pm$ 13	87 $\pm$ 2	0.100 <sup>4</sup>	No
E2	---	---	---	Yes

<sup>1</sup> Inhibition of the transformation of <sup>14</sup>C-E1 (60 nM) into <sup>14</sup>C-E2 by 17 $\beta$ -HSD1 in T-47D cells; <sup>2</sup> Proliferation of estrogen-sensitive T-47D cells. <sup>3</sup> IC<sub>50</sub> value from reference 7; <sup>4</sup> Estimated IC<sub>50</sub> value.

**Table 2.** Plasma PBRM concentrations and AUC values according to six vehicles and two modes of administration in female mice.<sup>1</sup>

Entry	Vehicles	Modes	Plasma concentration (ng/mL)						AUC (ng.h/mL)	
			3 h	5 h	7 h	9 h	12 h	24 h	0-7 h	0-24 h
1	MC/EtOH (92:8)	<i>sc</i>	412	478	342	186	96	65	2328	4244
	Whitening solution, ~ soluble	<i>po</i>	357	254	257	163	103	8	1656	3137
2	MC/DMSO (92:8)	<i>sc</i>	----	1167	1047	----	----	----	----	----
	Whitening solution, soluble	<i>po</i>	----	335	235	----	----	----	----	----
3	PG/EtOH (92:8)	<i>sc</i>	656	667	558	303	225	52	3531	6844
	Clear solution, soluble	<i>po</i>	195	172	248	42	155	31	1079	2776
4	PG/DMSO (92:8)	<i>sc</i>	----	----	708	----	----	----	----	----
	Clear solution, soluble	<i>po</i>	----	----	112	----	----	----	----	----
5	SO/EtOH (92:8)	<i>sc</i>	720	621	405	226	161	137	3448	6450
	Whitening solution, soluble	<i>po</i>	678	322	210	110	32	6	2549	3312
6	SO/DMSO (92:8)	<i>sc</i>	----	----	614	----	----	----	----	----
	clear solution, soluble	<i>po</i>	----	----	274	----	----	----	----	----

<sup>1</sup> PBRM was first dissolved in EtOH or DMSO and the solution added in aqueous 0.4% methyl cellulose (MC), propylene glycol (PG) or sunflower oil (SO) to obtain a final concentration of 250  $\mu$ g/100  $\mu$ L (14.7 mg/kg), which was subcutaneously (*sc*) or orally (*po*) administered in mice.

**Table 3.** Pharmacokinetic parameters calculated for PBRM following intravenous (*iv*) and subcutaneous (*sc*) administration in female mice.

Parameters	Mode of administration	
	<i>iv</i>	<i>sc</i>
Dose administered in mg/kg	2.0 <sup>1</sup>	14.7 <sup>2</sup>
<b>C<sub>max</sub></b> : maximum concentration recorded in ng/mL	873 <sup>3</sup>	990
<b>T<sub>max</sub></b> : time take to reach C <sub>max</sub> in h	NA	3
<b>AUC<sub>(0-7h)</sub></b> <i>iv</i> ; <b>AUC<sub>(0-12h)</sub></b> <i>sc</i> : area under the curve (in ng.h/mL)	1350	6210
<b>DNAUC<sub>(0-7h)</sub></b> <i>iv</i> ; <b>DNAUC<sub>(0-12h)</sub></b> <i>sc</i> : dose normalized AUC in (ng.h/mL)/(mg/kg)	674	422
<b>AUC<sub>(0-inf)</sub></b> : area under the concentration-time curve from zero up to $\infty$ with extrapolation of the terminal phase in ng.h/mL	1472	7042
<b>DNAUC<sub>(0-inf)</sub></b> : dose normalized AUC in (ng.h/mL)/(mg/kg)	736	480
<b>AUC %<sub>extrap</sub></b> : percent of AUC extrapolated beyond last time point	8.4	11.8
<b>T<sub>1/2</sub></b> : elimination half-life in h	2.2	3.4
<b>V<sub>z</sub></b> : volume of distribution during the terminal phase of <i>iv</i> administration in mL/kg	4270	10300 <sup>4</sup>
<b>CL</b> : clearance in mL/h.kg	1358	2088 <sup>4</sup>
<b>F</b> : absolute bioavailability in %	---	65

<sup>1</sup> PBRM administered in PG/DMA/DMSO (60:38:2); <sup>2</sup> PBRM administered in MC/DMSO (92:8); <sup>3</sup> Concentration at 0 h for *iv* dosing; <sup>4</sup> V<sub>z</sub>/F and CL/F values are presented.

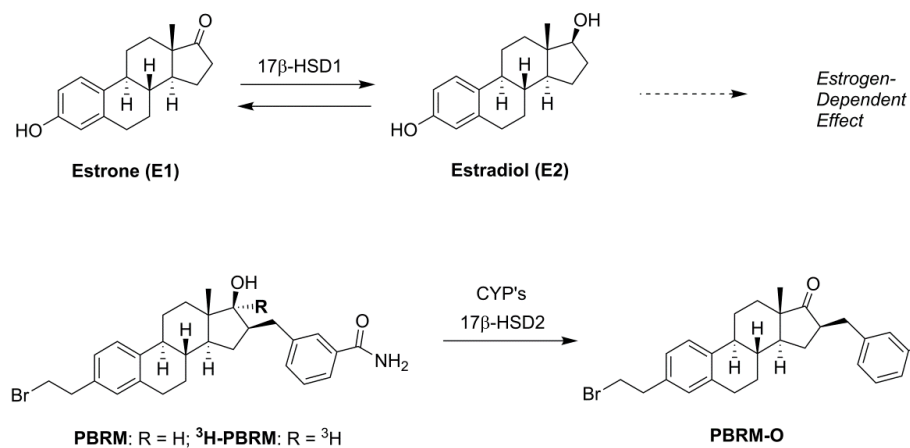


**Figure 1.** Conversion of E1 into the potent estrogen E2 by 17 $\beta$ -HSD1 (A) and representation of PBRM, <sup>3</sup>H-PBRM and PBRM-O (B).

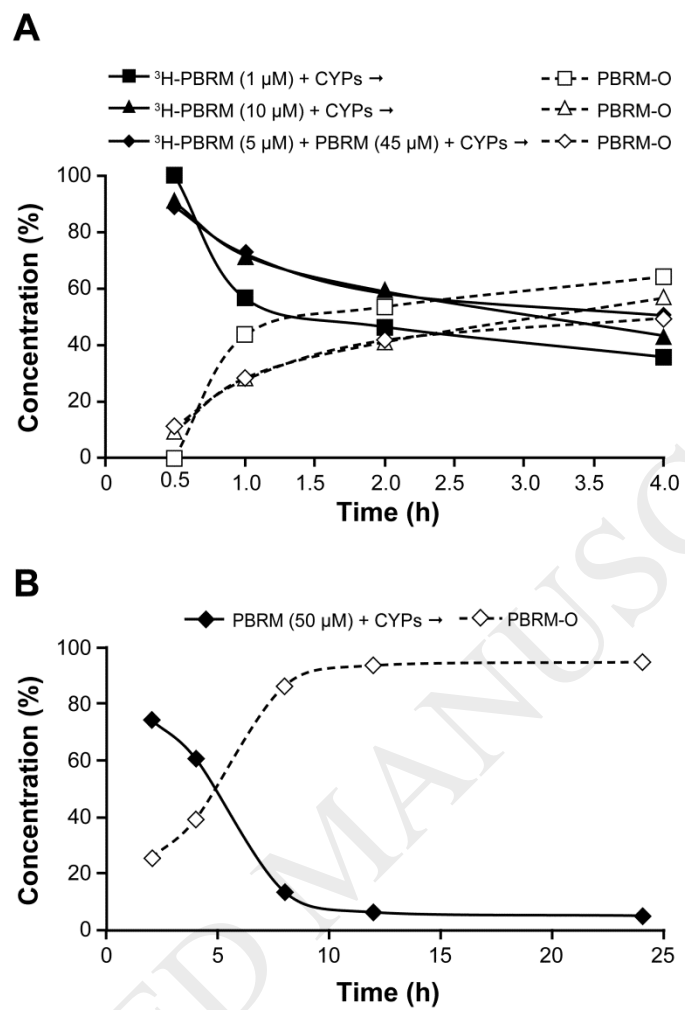


**Figure 2.** Metabolization of  $^3\text{H}$ -PBRM/PBRM during 0-4 h (**A**) or 0-24 h (**B**) in human liver microsomes showing a gradual conversion of PBRM to the oxidized metabolite PBRM-O.

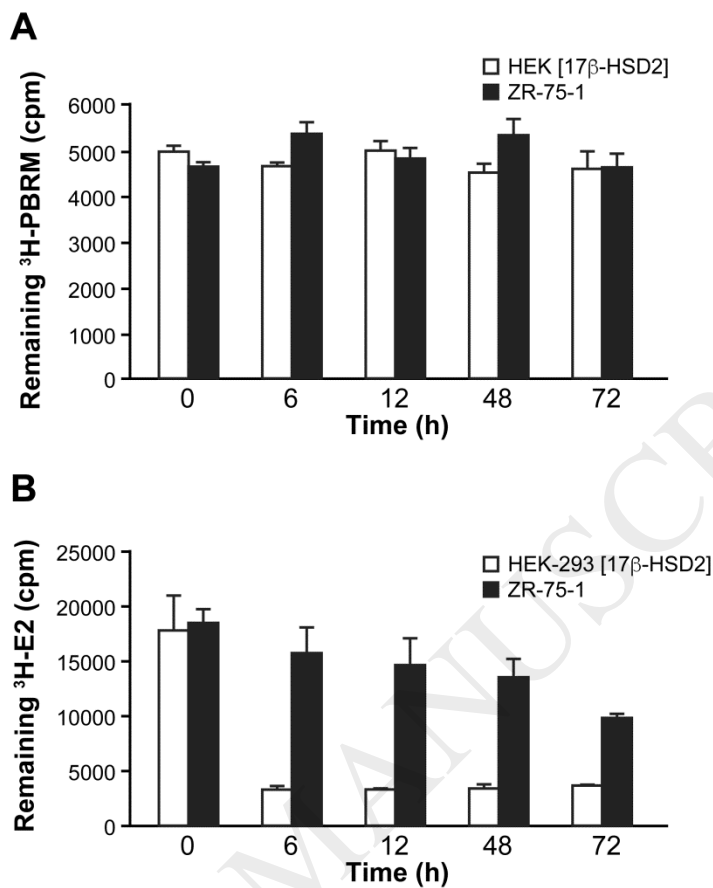


**Figure 3.** Disappearance of <sup>3</sup>H-PBRM in HEK-293[17β-HSD2] cells or ZR-75-1 cells (A) and disappearance of <sup>3</sup>H-E2 in HEK-293[17β-HSD2] cells or ZR-75-1 cells (B) following oxidation by 17β-HSD2.

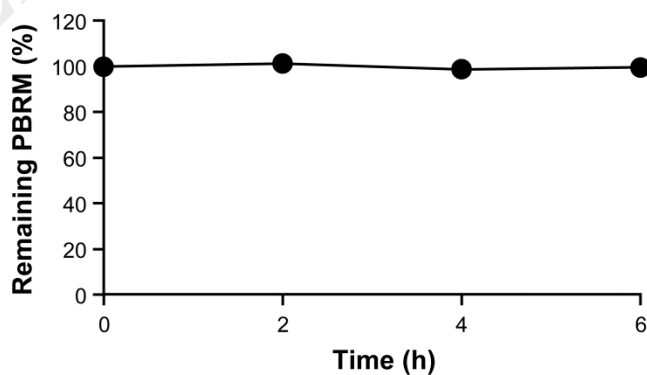


**Figure 4.** Stability of PBRM (5 μM) incubated in human plasma at 37 °C in function of time (0-6 h). The error bars (± SEM) are smaller than the symbols.

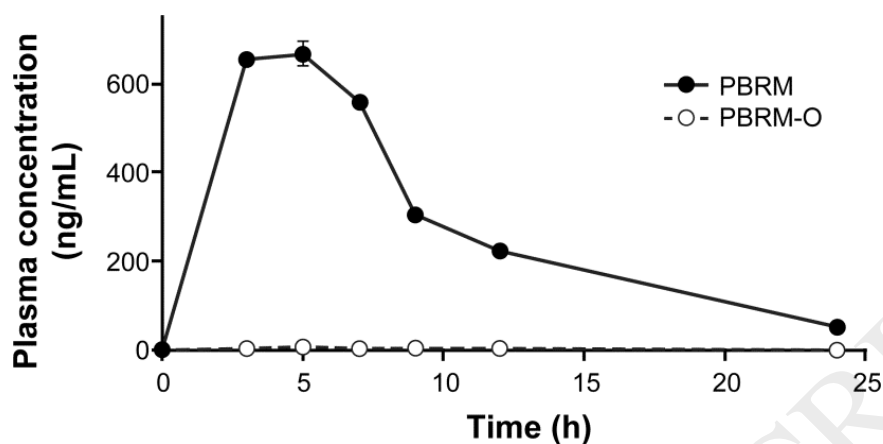


**Figure 5.** Plasma concentration of PBRM and PBRM-O following a single *sc* injection in female mice (2-3 per group) of PBRM (250  $\mu$ g in 100  $\mu$ L of PG/EtOH (92:8); 14.7 mg/kg). When the error bars ( $\pm$  SEM) are not shown, they are smaller than the symbols.

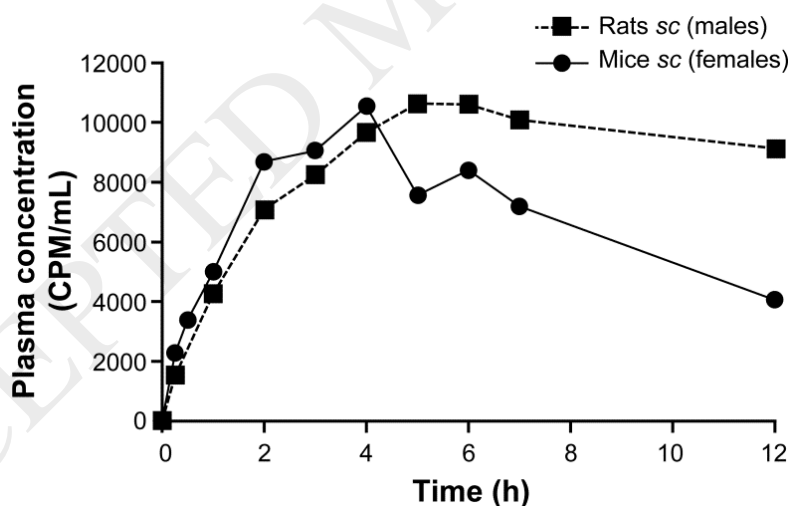


**Figure 6.** Plasma concentration of PBRM following a single *sc* injection in mice and rats (2-3 per group) of a mixture of  $^3$ H-PBRM/PBRM (0.3:99.7) at a dose of 14.7 mg/kg in MC/DMSO (92:8). The error bars ( $\pm$  SEM) are smaller than the symbols.

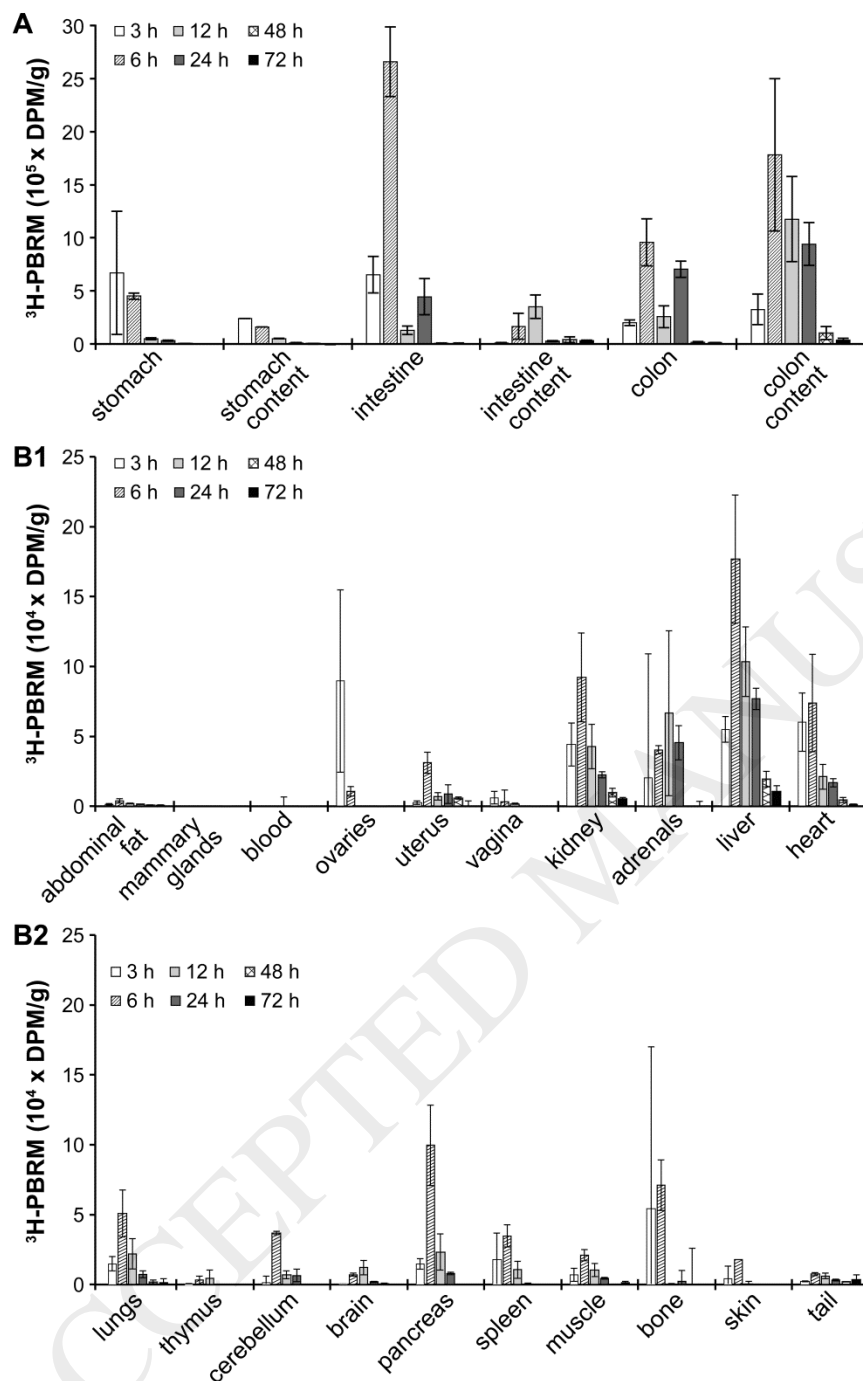


**Figure 7.** Tissue distribution of  $^3\text{H-PBRM}$  in the digestive track (**A**) and other tissues (**B1** and **B2**) of female mice. Three animals were sacrificed for each time after a single subcutaneous (*sc*) injection, and the organs were then collected, dissolved, and radioactivity quantified individually. The results are the mean value for three mice  $\pm$  SD. DPM: disintegrations per minute.



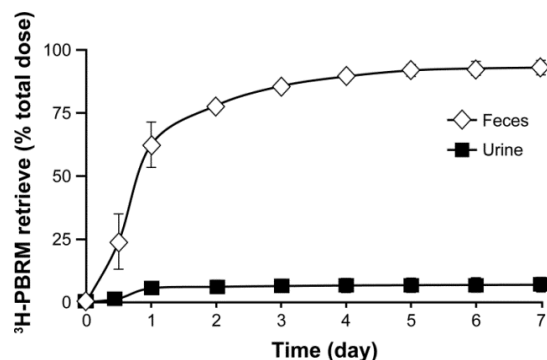


**Figure 8.** Mass balance of <sup>3</sup>H-PBRM injected *sc* in female mice. Feces and urine were recuperated, while cages were washed at determined times. The results are the mean  $\pm$  SD for two mice of the cumulative radioactivity measured in excrements in time, in terms of injected dose. When the error bars ( $\pm$  SEM) are not shown, they are smaller than the symbols.

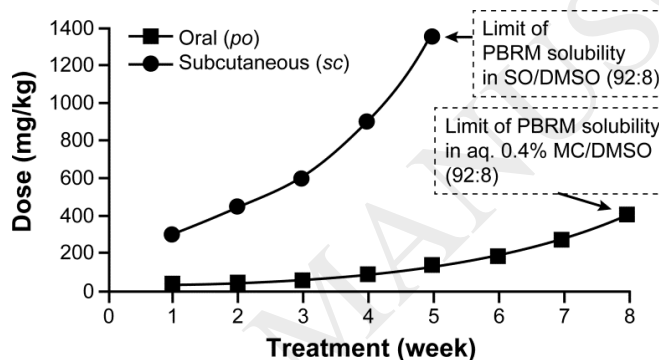


**Figure 9.** Determining the maximum tolerated dose of PBRM in female mice. Each week an increased dose of PBRM was given to each mouse (8 per group), and the signs of toxicity monitored daily. The PBRM doses are 30, 45, 60, 90, 135, 180, 270 and 405 mg/kg injected *sc* and 300, 450, 600, 900 and 1350 mg/kg administered by gavage (*po*).

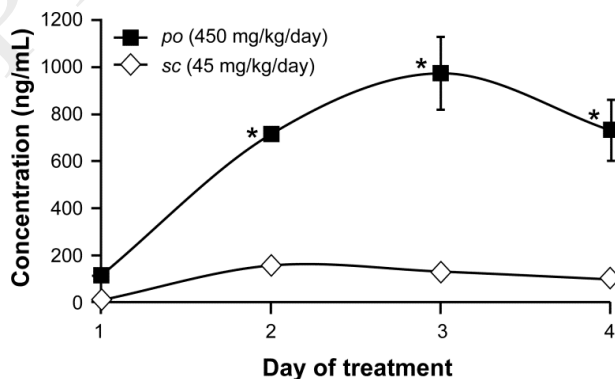


**Figure 10.** Accumulation of PBRM in female mouse plasma as a function of day of treatment and mode of administration (*sc* or *po*). The sampling was taken 24 h post-administration (2-4 mice per group). When the error bars ( $\pm$  SEM) are not shown, they are smaller than the symbols.

\* Data not significantly different between conditions (days 2, 3 and 4).